Superlattices and Microstructures 115 (2018) 191–196

Contents lists available at ScienceDirect

Superlattices and Microstructures

journal homepage: www.elsevier.com/locate/superlattices

Intermediate band formation in a δ-doped like QW superlattices of GaAs/$Al_xGa_{1-x}As$ for solar cell design

A. Del Río-De Santiago [a], J.C. Martínez-Orozco [b, *], K.A. Rodríguez-Magdaleno [b, c], D.A. Contreras-Solorio [b], I. Rodríguez-Vargas [b], F. Ungan [d]

[a] Unidad Académica de Ingeniería, Universidad Autónoma de Zacatecas, Ramón López Velarde 801, C.P. 98000 Zacatecas, Zac., Mexico
[b] Unidad Académica de Física, Universidad Autónoma de Zacatecas, Calzada Solidaridad esquina con Paseo la Bufa S/N, C.P. 98060 Zacatecas, Zac., Mexico
[c] Centro de Investigación en Ciencias, IICBA, Universidad Autónoma del Estado de Morelos, Av. Universidad 1001, C.P. 62209 Cuernavaca, Morelos, Mexico
[d] Faculty of Technology, Department of Optical Engineering, Cumhuriyet University, 58140 Sivas, Turkey

ARTICLE INFO

Article history:
Received 9 January 2018
Accepted 27 January 2018
Available online 22 February 2018

Keywords:
δ-doped superlattice
Intermediate-band
Solar cells

ABSTRACT

It is reported a numerical computation of the local density of states for a δ-doped like QW superlattices of $Al_xGa_{1-x}As$, as a possible heterostructure that, being integrated into a solar cell device design, can provide an intermediate band of allowed states to assist the absorption of photons with lower energies than that of the energy gap of the solar-cell constituent materials. This work was performed using the nearest neighbors sp^3s^* tight-binding model including spin. The confining potential caused by the ionized donor impurities in δ-doped impurities seeding that was obtained analytically within the lines of the Thomas-Fermi approximation was reproduced here by the Al concentration x variation. This potential is considered as an external perturbation in the tight-binding methodology and it is included in the diagonal terms of the tight-binding Hamiltonian. Special attention is paid to the width of the intermediate band caused by the change in the considered aluminium concentration x, the inter-well distance between δ-doped like QW wells and the number of them in the superlattice. In general we can conclude that this kind of superlattices can be suitable for intermediate band formation for possible intermediate-band solar cell design.

1. Introduction

The intermediate-band solar cell (IBSC) has been proposed originally by A. Luque and A. Martí [1] as a system whose reported theoretical conversion efficiency can exceed the Shockley and Queisser model (SQM) limiting value of 40.7% [2] for *p-n* junction solar cells. In fact A. Luque and A. Martí reported a theoretical efficiency of about 60.3% when the intermediate band mechanism is considered, this can explain why the pursuit of an efficient mechanism for the intermediate band formation is on the table [3–8]. This mechanism consists in the existence of an accessible intermediate energy band that splits the otherwise conventional semiconductor bandgap into two, that enable the absorption of photons with lesser energy than that of the energy gap. On these devices a photocurrent is produced when the solar cell is illuminated with below band-gap

* Corresponding author.
E-mail address: jcmartinez@uaz.edu.mx (J.C. Martínez-Orozco).

https://doi.org/10.1016/j.spmi.2018.01.029
0749-6036/

energy photons. In this paper we present a semi-empirical numerical computation to show that the two main principles of operation required by the IBSC are fulfilled, meaning that the exciton between the valence and the conduction band is present and that the absorption of photons from the valence band to the intermediate band and absorption of them from the intermediate band to the conduction one could also be present through the intermediate band, this is the named two-step photon absorption mechanism. From the approach of an intermediate-band (IB) generated by a δ-doped like quantum well superlattice (QW SLs), of which we provide a geometry and number of wells appropriated for a possible solar-cell feasible design by epitaxial growth method.

In 2006 A. Martí et al. experimentally demonstrated that the two-step photon absorption mechanism is possible, in fact they measured the photon absorption from the valence band to the IB and from this last one to the conduction band on a quantum dot solar cell [9]. Recently, there has been also important efforts from several authors in order to explain in great detail this mechanism as well as its progress and perspectives [10–12]. In particular, this mechanism is being widely investigated in quantum dots for its theoretical predicted solar photon conversion up to about 66% [13]. There has been theoretical studies for the intermediate band formation for GaAs/Al_xGa_{1-x}As multi-shell quantum dots as a function of size distributions [14] and its intra-miniband absorption coefficient [15], optical properties of CdSe/ZnS core/shell quantum dots layers analyzing its application to photovoltaic solar cells [16], and modeling of the interminiband absorption coefficient in InGaN cuboid shape quantum dot superlattices [17], among others studies [18–23].

On the other hand, the δ-doping profile is probably an important system to produce an IBSC device, this single atomic-layer high-impurity seeding of doping impurities is possible due to the molecular beam epitaxy [24] and the first δ-doped superlattice in III-V semiconductors, with Be as p-type and Si as n-type δ-doping, was carried out by K. Ploog [25], but in fact the very early superlattice was established by L. Esaki and R. Tsu [26]. Recently, with the reached control on this growth technique, in different semiconductor materials, the Nitrogen δ-doped AlGaAs superlattices has been recently studied experimentally by several authors for IBSC applications [27–37], among other studies it has been included photoluminescence measurements [30,34], and photoreflectance [35], some authors proposed the improving of the efficiency in intermediate band solar cells by the overlapping absorptions [36] especially for intermediate bands that are near the middle of the bandgap. In fact, T. Suzuki et al. [37] fabricated a GaAs:N δ-doped QW superlattices by molecular beam epitaxy and demonstrated that the two-step photon absorption process for an IB Solar Cell was possible but under additional infrared illumination at room temperature, as already was demonstrated by Martí et al. in the case of quantum dot solar cell [9], the advantage of δ-doped QW superlattice could be that, in principle, it is easier to growth than quantum dot solar cell. From the theoretical point of view, there has been also some papers that analyzes the miniband formation in n-type δ-doped GaAs finite superlattice [38] and miniband formation in parabolic GaAs/Al_xGa_{1-x}As superlattices [39] under the semi-empirical tight-binding approximation. In this line, the tight-binding approach demonstrated to be suitable to investigate also some three dimensional band structures for III-V layer compounds as GaSe and InSe [40]. So, in the present paper we analyze the intermediate band formation in a δ-doped like QW GaAs/Al_xGa_{1-x}As superlattices for solar cell design within the nearest neighbors sp^3s^* tight-binding model including spin. This potential is considered as an external perturbation in the tight-binding methodology, and it is added to the diagonal terms of the tight-binding Hamiltonian. Detailed information of the miniband structure formation as a function of the aluminium concentration and the space layer is given.

The structure of the paper is as follows: In Section 2 we present the theoretical model and the system description. In Section 3 the corresponding results and discussions. Finally, in Section 4 we present the main findings and conclusions of our study.

2. Theoretical model

In this paper we implemented a semi-empirical tight-binding method by considering first nearest neighbors with a spin dependent sp^3s^* basis, using the Green function formalism and the Surface Green Function Matched (SGFM) method, in order to compute the Local Density of States (LDOS) for an external potential along the (001) direction. This computation is performed adding the discretized external potential in each layer of the diagonal elements of the Hamiltonian matrix. This method originally was used to consider static externally applied electric and magnetic fields and generalized later by M. Graf and P. Vogl to time dependent electromagnetic fields [41], the advantage of this methodology is that there is not necessary any extra adjustable tight-binding system parameters. In the case of a single δ-doped like quantum well S. Vlaev and L. M. Gaggero-Sager [42] solved, by this method, the potential given by Ioratti's self consistent solution [43], reporting correct results. In this paper we are interested in a δ-doped like QW superlattice (SLs), depicted in Fig. 1, with the δ-doped like QW potential given by Ioratti's potential [43].

$$V_{QW}(z) = -\frac{\alpha^2}{(\alpha|z| + z_0)^4} \tag{1}$$

being $\alpha = 2/15\pi$ and $z_0 = (\alpha^3/\pi N_{2D})^{1/5}$, with N_{2D} that represents the two-dimensional impurities density that will generate the band bending in the single δ-doped QW. In fact in this work we model the δ-doped like QW SLs via the aluminium concentration $x(z)$, as a function of the system growth direction coordinate z. Here we must stress that we need to discretize the continuous variable z with a new discrete variable n, that label the atomic layer in the growth direction, in order to

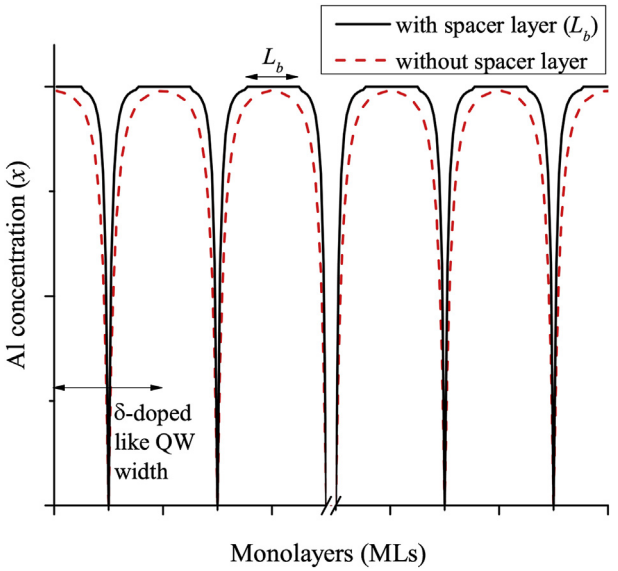

Fig. 1. Schematic representation of a δ-doped like QW SL. The single δ-doped quantum well depth is determined by the aluminium concentration (x) while the δ-doped well width depends on the number of MLs that we are considering (represented by double ended-arrow line). The segmented-line stands for adjacent δ-doped like QW, while the solid line considers a spacer layer (L_b) characterized by flat potential regions.

reconstruct the δ-doped like QW potential profile as a function of the aluminium concentration (x), as proposed in Ref. [42]. So the corresponding expression for $V_{SL}(z)$ in the superlattice is constructed with a suitable combination of single δ-doped like QW potential functions (see Fig. 1) and it is incorporated to the diagonal terms of the tight-binding Hamiltonian,

$$TB_{ii}(n) = TB_{ii}(0) + V(n), \tag{2}$$

where the potential $V(n)$ is the superlattice potential $V_{SL}(z)$ written in the discrete coordinates n that label each atomic layer in monolayers MLs, together with SGFM method at the center of the Brillouin zone for the (001) growth direction. For the parameters of the $Al_xGa_{1-x}As$ alloy, we use the virtual cristal approximation.

3. Results and discusion

In this paper we are studying the intermediate band formation in a $GaAs/Al_xGa_{1-x}As$ system as a function of the number of δ-doped like QW in the finite SLs located in the GaAs region, in this region the aluminium concentration determinate the depth of the QW and the number of MLs of the well as well as the effect of the spacer layer determinate the QW width. In particular, we consider the parameters used by T. Suzuki et al. [37] in order to compare our results and to discuss about of the importance of the spacer layer in the intermediate band formation, T. Suzuki et al. reported a 20-period δ-doped superlattice within $Al_{0.2}Ga_{0.8}As$ layers in both sides as carrier blocking layers. The tight-binding matrix parameters are the ones reported by Boykin et al., that in fact correctly reproduce the effective masses of the constituent materials [44].

In Fig. 2 a) we present the density of states for GaAs (black solid-line), for the $Al_xGa_{1-x}As$ with $x = 0.2$ (red dashed-line) and $x = 0.3$ (blue dash-dot-line), and finally the green line (light-green filled) stands for the density of states of a succession of 21 δ-doped like QW, with an aluminium concentration of $x = 0.1$ that gives a QW depth of about 93.1 meV, considering 20 MLs spacers (see Fig. 1 flat region). The computed values of the gaps, for T = 0, are 1993 meV for $x = 0.3$, 1845 meV for $x = 0.2$ and 1552 meV for GaAs, that are in good agreement with previous computed results [45]. We find the formation of an intermediate band, of width of 14 meV, between the CB of the GaAs and the $Al_{0.2}Ga_{0.8}$ As band offset, with an energy E_- of 85 meV, defined as the difference of the miniband minimum and the bottom of the GaAs CB, and an E_+ value of about 89 meV, defined as the difference on the $Al_{0.2}Ga_{0.8}$ As CB border and the maximum value on the miniband. In Fig. 2 b) we show, by restricting the energy axis to the CB energy region, the DOS for arrays of 11, 21, 31 δ-doped like QW with 20 MLs spacers, and find that the intermediate band width is practically the same in the three cases and it is probably one of the most interesting results of this study, which leads us to propose that 11 δ-doped like QWs are enough to observe SLs behavior and avoid growth with more QW wells which is complicated from the experimental point of view.

Once we know that the miniband can be produced by a δ-doped like QW SLs, we wonder what it takes to move this intermediate band between the CBs of the $GaAs/Al_{0.2}Ga_{0.8}$ As heterostructure for the possible design of an intermediate-band solar-cell (IBSC) active region or how to vary the width of the miniband, so in Fig. 3 a) we studied the intermediate band for the system as a function of the $Al_{0.2}Ga_{0.8}$ As spacer layer, characterized by the parameter L_b in MLs, fixing the δ-doped like QW

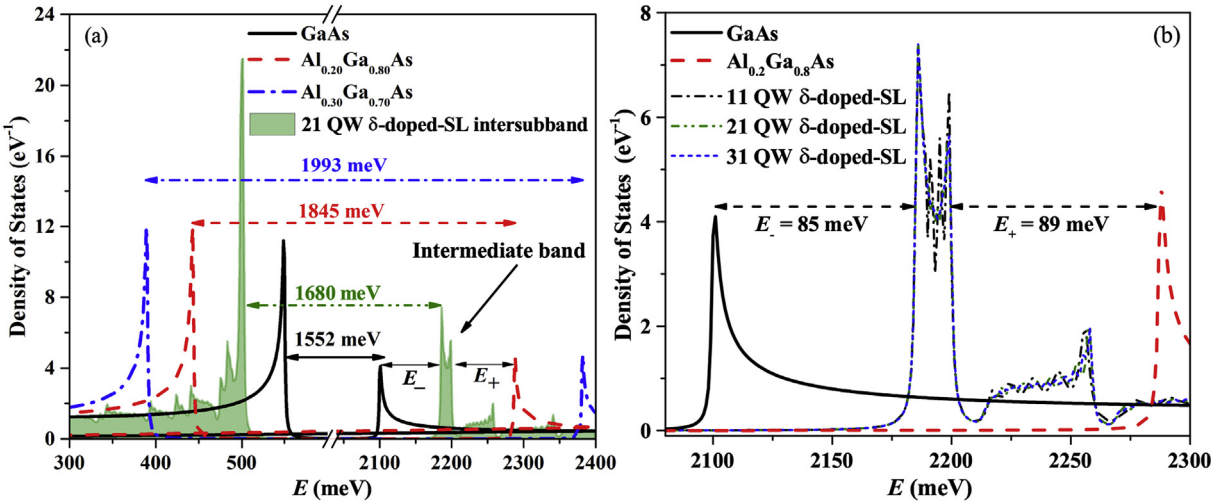

Fig. 2. a) Density of states DOS for GaAs and $Al_xGa_{1-x}As$ for $x = 0.2$ and 0.3 as well as for a 21 δ-doped like QW superlattice (intermediate band generation), the computed band gaps are depicted for each aluminium concentration. In b) we restrict the energy axis to the conduction bands region and reported the DOS for 11, 21 and 31 δ-doped-SL considering a 20 MLs spacers with an aluminium concentration of $x = 0.1$ for the δ-doped like QWSLs in the GaAs region that induces the miniband formation, of width of 14 meV, the E_- and E_+ are also depicted.

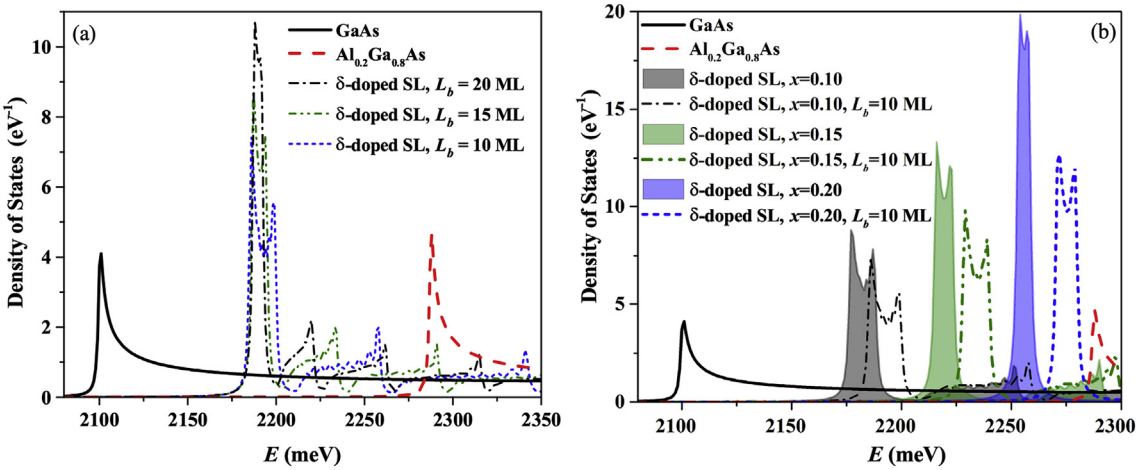

Fig. 3. a) Density of states for a 21 δ-doped like QW SLs considering an aluminium concentration of $x = 0.1$ as we decrease the spacer layer width for $L_b = 20, 15$ and 10 MLs. And, b) as we increase the aluminium concentration for the δ-doped like QW profile of the finite SLs for $x = 0.1$, 0.15 y 0.2 with (segmented-lines) and without (continuous-line filled-area) spacer layer of $L_b = 10$ MLs.

aluminium concentration to $x = 0.1$ and the whole well width to 40 MLs, here we considered $L_b = 20$, 15 and 10 MLs and we find that the FWHM are 7, 10 and 15 meV, respectively, that is an expected behavior because when the spacer layer is narrower the ground state wave function of each individual δ-doped like QW overlap more and the intermediate-band is wider (short-dashed blue-line), that means that a narrower spacer layer gives a wider intermediate-band width. In Fig. 3 b) we compare whether the spacer layer, of 10 MLs on both sides of the δ-doped like QWs, is considered or not as well as different δ-doped like QW aluminium concentration of $x = 0.1$, 0.15 and 0.2. In general, as the aluminium concentration increases, the intermediate-band recedes further from the GaAs conduction band bottom as get close to the $Al_{0.2}Ga_{0.8}$ As CB border and, when in the system the 10 MLs spacer layer is considered, the intermediate-band is closest compared with the case of the SLs without any spacer layer and the intermediate-band width is wider. So this represent an efficient way to manipulate the intermediate-band width and relative position to design IBSCs with δ-doped like QW SLs.

Finally, in Fig. 4 we present the density of states for a 21 δ-doped like QW SLs surrounded by semi-infinite $Al_{0.2}Ga_{0.8}$ As external barriers (carrier blocking layers), because in all the previous cases we did not consider this extra confinement mechanism, that indeed is part of the solar cell design. In this case we considered three different Al concentrations to generate the δ-doped like QW SLs: $x = 0.10$, 0.15 and 0.20. In the former case the difference, in concentration, from the external barrier height to the top of the 21 δ-doped like QW SLs (depicted in Fig. 1) is $x = 0.10$, in the second case is $x = 0.5$, and in the last case

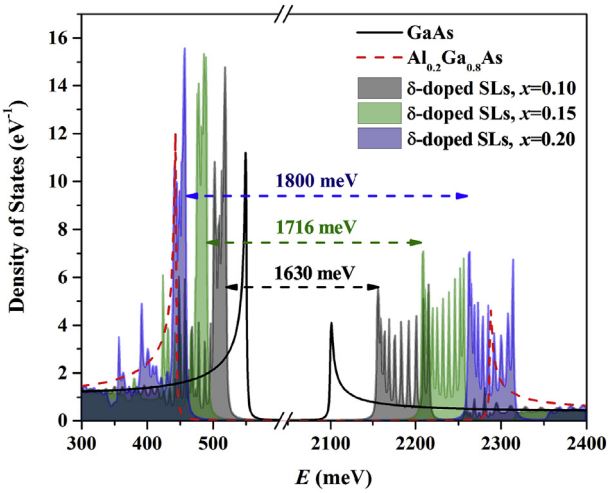

Fig. 4. Density of states for a 21 δ-doped like QW SLs surrounded by $Al_{0.2}Ga_{0.8}As$ external barriers. Here we reported the valence and conduction band shift as a function on the Al concentration of the δ-doped like QW as we increasing the aluminium concentration for the δ-doped like QW profile of the SLs for $x = 0.10$, 0.15 y 0.2.

there is no difference in the aluminium concentration but still is active the confinement effect of barriers. Contrary to the previous cases here we also calculate the DOS considering the energy range of the valence band and for the case of $x = 0.10$ we find an energy gap between the valence-conduction band intra-subband is of 1630 meV and in general we can observe that as we increase the Al concentration the BV-CB intra-subband energy gap increases. In this figure we also depicted the GaAs and $Al_{0.2}Ga_{0.8}$ As DOS in order to see the relative position of the generated intermediate band in the system.

4. Conclusions

In summary we reported a tight-binding computation for the electronic structure of δ-doped QW SL considering 11, 21 and 31 δ-doped like QWs and aluminium concentration of $x = 0.1$, 0.15 and 0.2, with external barrier of $Al_xGa_{1-x}As$ with the same Al concentration, as well as the effect of spacer layer between δ-doped like QW. In particular we find that for an array for 11 δ-doped like QW, and $x = 0.1$, we have a well defined CB intermediate band, so in principle it is not necessary to growth a SLs with more than 11 δ-doped like QW, because the computed local density of states is practically the same than for 21 and 31. We also find that it is possible to manipulate the width of the intermediate band with the implementation of different spacer layers widths (L_b), and if we increase the aluminium concentration, that determinate de δ-doped like QW depth, the intermediate band position can be also shifted. Finally we also implemented a semi-infinite $Al_{0.2}Ga_{0.8}As$ external barriers (carrier blocking layers) as an extra confinement mechanism and demonstrated that intra-subband energy gap from the VB intermediate band to the CB intermediate band can be modified by changing the Al concentration for the δ-doped like QW SL, this particular result could be exploited to design a tandem solar cell, for instance, the top one with a 21 δ-doped like QW and Al concentration of $x = 0.2$ that has a direct energy gap of about 1800 meV and then another one with $x = 0.15$ that has an energy gap of 1716 meV and finally the one with $x = 0.1$ that has an even smaller energy gap, that is the principle of tandem solar cells. Then we demonstrated that the δ-doped like QW SLs potential profile could be an important mechanism to form the intermediate band for its implementation in IBSC.

Appendix A. Supplementary data

Supplementary data related to this article can be found at https://doi.org/10.1016/j.spmi.2018.01.029.

References

[1] A. Luque, A. Martí, Increasing the efficiency of ideal solar cells by photon induced transitions at intermediate levels, Phys. Rev. Lett. 78 (1997), 5014, https://doi.org/10.1103/PhysRevLett.78.5014.
[2] W. Shockley, H.J. Queisser, Detailed balance limit of efficiency of p-n junction solar cells, J. Appl. Phys. 32 (1961) 510, https://doi.org/10.1063/1.1736034.
[3] N.S. Beattie, P. See, G. Zoppi, P.M. Ushasree, M. Duchamp, I. Farrer, D.A. Ritchie, S. Tomić, Quantum engineering of InAs/GaAs quantum dot based intermediate band solar cells, ACS Photonics 4 (2017) 2745, https://doi.org/10.1021/acsphotonics.7b00673.
[4] J.E. Castellanos-Águila, P. Palacios, J.C. Conesa, J. Arriaga, P. Wahnón, Theoretical band alignment in an intermediate band chalcopyrite based material, Appl. Surf. Sci. 424 (2017) 132, https://doi.org/10.1016/j.apsusc.2016.12.237.
[5] Y. Kim, I.-W. Cho, M.-Y. Ryu, J.O. Kim, S.J. Lee, K.-Y. Ban, C.B. Honsberg, Stranski–Krastanov InAs/GaAsSb quantum dots coupled with sub-monolayer quantum dot stacks as a promising absorber for intermediate band solar cells, Appl. Phys. Lett. 111 (2017), 073103, https://doi.org/10.1063/1.4999437.

[6] I. Ramiro, J. Villa, C. Tablero, E. Antolín, A. Luque, A. Martí, J. Hwang, J. Phillips, A.J. Martin, J. Millunchick, Analysis of the intermediate-band absorption properties of type-II GaSb/GaAs quantum-dot photovoltaics, Phys. Rev. B 96 (2017), 125422, https://doi.org/10.1103/PhysRevB.96.125422.

[7] J. Yuan, H. Huang, X. Deng, M. Gong, C. Liu, Z. Yue, C. Gao, N. Zhou, L. Zhou, Intermediate band materials obtained by rapid thermal process of Co-implanted silicon, Mater. Lett. 209 (2017) 522–524, https://doi.org/10.1016/j.matlet.2017.08.095.

[8] K. Zelazna, M. Gladysiewicz, M.P. Polak, S. Almosni, A. Létoublon, C. Cornet, O. Durand, W. Walukiewicz, R. Kudrawiec, Nitrogen-related intermediate band in P-rich $GaN_xP_yAs_{1-x-y}$ alloys, Sci. Rep-UK 7 (2017) 15703, https://doi.org/10.1038/s41598-017-15933-1.

[9] A. Martí, E. Antolín, C.R. Stanley, C.D. Farmer, N. López, P. Díaz, E. Cánovas, P.G. Linares, A. Luque, Production of photocurrent due to intermediate-to-conduction-band transitions: a demonstration of a key operating principle of the intermediate-band solar cell, Phys. Rev. Lett. 97 (2006) 247701, https://doi.org/10.1103/PhysRevLett.97.247701.

[10] A. Luque, A. Martí, The intermediate band solar cell: progress toward the realization of an attractive concept, Adv. Mater. 22 (2010) 160, https://doi.org/10.1002/adma.200902388.

[11] A. Luque, A. Martí, C. Stanley, Understanding intermediate-band solar cells, Nat. Photon. 6 (2012) 146, https://doi.org/10.1038/nphoton.2012.1.

[12] Y. Okada, N.J. Ekins-Daukes, T. Kita, R. Tamaki, M. Yoshida, A. Pusch, O. Hess, C.C. Phillips, D.J. Farrell, K. Yoshida, N. Ahsan, Y. Shoji, T. Sogabe, J.-F. Guillemoles, Intermediate band solar cells: recent progress and future directions, Appl. Phys. Rev. 2 (2015) 021302, https://doi.org/10.1063/1.4916561.

[13] A.J. Nozik, Quantum dot solar cells, Physica E 14 (2002) 115, https://doi.org/10.1016/S1386-9477(02)00374-0.

[14] K.A. Rodríguez-Magdaleno, R. Pérez-Álvarez, J.C. Martínez-Orozco, R. Pernas-Salomón, Multi-shell spherical GaAs/AlxGa^{1-x}As quantum dot shells-size distribution as a mechanism to generate intermediate band energy levels, Physica E 88 (2017) 142, https://doi.org/10.1016/j.physe.2017.01.007.

[15] K.A. Rodríguez-Magdaleno, R. Pérez-Álvarez, J.C. Martínez-Orozco, Intra-miniband absorption coefficient in GaAs/Al_xGa_{1-x}As core/shell spherical quantum dot, J. Alloy. Comp. 736 (2018) 211, https://doi.org/10.1016/j.jallcom.2017.11.091.

[16] H.-J. Lin, S. Vedraine, J. Le-Rouzo, S.-H. Chen, F. Flory, C.-C. Lee, Optical properties of quantum dots layers: application to photovoltaic solar cells, Sol. Energy Mater. Sol. Cells 117 (2013) 652, https://doi.org/10.1016/j.solmat.2012.12.005.

[17] G. Giannoccaro, F.D. Leonardis, V.M.N. Passaro, Modeling of the interminiband absorption coefficient in InGaN quantum dot superlattices, Photonics 3 (2016) 5, https://doi.org/10.3390/photonics3010005.

[18] I. Bragar, P. Machnikowski, Intraband absorption in finite, inhomogeneous quantum dot stacks for intermediate band solar cells: limitations and optimization, J. Appl. Phys. 112 (2012), 124318, https://doi.org/10.1063/1.4770383.

[19] T. Nozawa, Y. Arakawa, Matrix elements of intraband transitions in quantum dot intermediate band solar cells: the influence of quantum dot presence on the extended-state electron wave-functions, Semicond. Sci. Technol. 29 (2014), 045014, https://doi.org/10.1088/0268-1242/29/4/045014.

[20] S. Huang, A.V. Semichaevsky, L. Webster, H.T. Johnson, R.S. Goldman, Influence of wetting layers and quantum dot size distribution on intermediate band formation in InAs/GaAs superlattices, J. Appl. Phys. 110 (2011), 073105, https://doi.org/10.1063/1.3631785.

[21] J. Wu, D. Shao, Z. Li, M.O. Manasreh, V.P. Kunets, Z.M. Wang, G.J. Salamo, Intermediate-band material based on GaAs quantum rings for solar cells, Appl. Phys. Lett. 95 (2009), 071908, https://doi.org/10.1063/1.3211971.

[22] A. Luque, A. Martí, N. López, E. Antolín, E. Cánovas, C. Stanley, C. Farmer, L.J. Caballero, L. Cuadra, J.L. Balenzategui, Experimental analysis of the quasi-Fermi level split in quantum dot intermediate-band solar cells, Appl. Phys. Lett. 87 (2005), 083505, https://doi.org/10.1063/1.2034090.

[23] P.V. Kamat, Quantum dot solar cells. Semiconductor nanocrystals as light harvesters, J. Phys. Chem. C 112 (2008), 18737, https://doi.org/10.1021/jp806791s.

[24] C.E.C. Wood, G. Metze, J. Berry, L.F. Eastman, Complex free-Carrier profile synthesis by "atomic-plane" doping of MBE GaAs, J. Appl. Phys. 51 (1980) 383, https://doi.org/10.1063/1.327383.

[25] K. Ploog, Molecular beam epitaxy of artificially layered III-V semiconductors: ultrathin-layer $(GaAs)_m$ $(AlAs)_m$ superlattices and delta (δ-) doping in GaAs, Phys. Scripta 1987 (T19A) (1987) 136.

[26] L. Esaki, R. Tsu, Superlattice and negative differential conductivity in semiconductors, IBM J. Res. Dev. 14 (1970) 61, https://doi.org/10.1147/rd.141.0061.

[27] S. Yagi, S. Noguchi, Y. Hijikata, S. Kuboya, K. Onabe, Y. Okada, H. Yaguchi, Enhanced optical absorption due to E_+ -related band transition in GaAs:N δ-doped superlattices, Appl. Phys. Express 7 (2014), 102301, https://doi.org/10.7567/APEX.7.102301.

[28] S. Yagi, S. Noguchi, Y. Hijikata, S. Kuboya, K. Onabe, H. Yaguchi, Conversion efficiency of intermediate band solar cells with GaAs:N δ-doped superlattices, Jpn. J. Appl. Phys. 52 (2013), 102302, https://doi.org/10.7567/JJAP.52.102302.

[29] K. Osada, T. Suzuki, S. Yagi, S. Naitoh, Y. Shoji, Y. Hijikata, Y. Okada, H. Yaguchi, Control of intermediate-band configuration in GaAs:N δ-doped superlattice, Jpn. J. Appl. Phys. 54 (2015), 08KA04, https://doi.org/10.7567/JJAP.54.08KA04.

[30] F. Ishikawa, S. Furuse, K. Sumiya, A. Kinoshita, M. Morifuji, Nitrogen δ-doping for band engineering of GaAs-related quantum structures, J. Appl. Phys. 111 (2012), 053512, https://doi.org/10.1063/1.3691239.

[31] S. Noguchi, S. Yagi, D. Sato, Y. Hijikata, K. Onabe, S. Kuboya, H. Yaguchi, Analysis of electronic structures of nitrogen δ-doped GaAs superlattices for high efficiency intermediate band solar cells, IEEE J. Photovolt 3 (2013) 1287, https://doi.org/10.1109/JPHOTOV.2013.2271978.

[32] Y. Ogawa, Y. Harada, T. Baba, T. Kaizu, T. Kita, Effects of rapid thermal annealing on two-dimensional delocalized electronic states of the epitaxial N δ-doped layer in GaAs, Appl. Phys. Lett. 108 (2016), 111905, https://doi.org/10.1063/1.4944055.

[33] E. Luna, R. Gargallo-Caballero, F. Ishikawa, A. Trampert, Morphological and chemical instabilities of nitrogen delta-doped GaAs/(Al, Ga)As quantum wells, Appl. Phys. Lett. 110 (2017), 201906, https://doi.org/10.1063/1.4983837.

[34] S.-I. Furuse, K. Sumiya, M. Morifuji, F. Ishikawa, Molecular beam epitaxial growth and characterization of nitrogen δ-doped AlGaAs/GaAs quantum wells, J. Vac. Sci. Technol. B 30 (2012), 02B117, https://doi.org/10.1116/1.3678204.

[35] K. Sumiya, M. Morifuji, Y. Oshima, F. Ishikawa, formation of minibands on superlattice structure with periodically arranged δ-doped nitrogen into GaAs, Appl. Phys. Express 6 (2013), 041002, https://doi.org/10.7567/APEX.6.041002.

[36] A. Krishna, J.J. Krich, Increasing efficiency in intermediate band solar cells with overlapping absorptions, J. Optic. 18 (2016), 074010, https://doi.org/10.1088/2040-8978/18/7/074010.

[37] T. Suzuki, K. Osada, S. Yagi, S. Naitoh, Y. Shoji, Y. Hijikata, Y. Okada, H. Yaguchi, Molecular beam epitaxial growth of intermediate-band materials based on GaAs:N δ-doped superlattices, Jpn. J. Appl. Phys. 54 (2015), 08KA07, https://doi.org/10.7567/JJAP.54.08KA07.

[38] I. Rodríguez-Vargas, J. Madrigal-Melchor, S.J. Vlaev, Miniband structure analysis of n-type delta-doped GaAs superlattices, Rev. Mexic. Fisica S. 53 (2007) 106.

[39] I. Rodríguez-Vargas, O.Y. Sánchez-Barbosa, D.A. Contreras-Solorio, S.J. Vlaev, Miniband structure of parabolic superlattices, Microelectron. J. 39 (2008) 423, https://doi.org/10.1016/j.mejo.2007.07.060.

[40] M.O.D. Camara, A. Mauger, I. Devos, Electronic structure of the layer compounds GaSe and InSe in a tight-binding approach, Phys. Rev. B 65 (2002) 125206, https://doi.org/10.1103/PhysRevB.65.125206.

[41] M. Graf, P. Vogl, Electromagnetic fields and dielectric response in empirical tight-binding theory, Phys. Rev. B 51 (1995) 4940, https://doi.org/10.1103/PhysRevB.51.4940.

[42] S. Vlaev, L.M. Gaggero-Sager, Thomas-Fermi approximation in a tight-binding calculation of δ-doped quantum wells in GaAs, Phys. Rev. B 58 (1998) 1142, https://doi.org/10.1103/PhysRevB.58.1142.

[43] L. Ioriatti, Thomas-Fermi theory of δ-doped semiconductor structures: exact analytical results in the high-density limit, Phys. Rev. B 41 (1990) 8340, https://doi.org/10.1103/PhysRevB.41.8340.

[44] T.B. Boykin, G. Klimeck, R.C. Bowen, R. Lake, Effective-mass reproducibility of the nearest-neighbor sp^3s^* models: analytic results, Phys. Rev. B 56 (1997) 4102, https://doi.org/10.1103/PhysRevB.56.4102.

[45] P. Vogl, H.P. Hjalmarson, J.D. Dow, A semi-empirical tight-binding theory of the electronic structure of semiconductors, J. Phys. Chem. Solid. 44 (1983) 365, https://doi.org/10.1016/0022-3697(83)90064-1.